The Origin of Electrocatalytic Activity of Gold Nanoparticles Modified Pt-Based Surfaces Towards Formic Acid Oxidation

Gumaa A. El-Nagar, Ahmad M. Mohammad, Mohamed S. El-Deab and Bahgat E. El-Anadouli

Abstract Recently, direct formic acid fuel cells (DFAFCs) have received much attention in both industry and academia, due to their unique properties. Despite of their broad benefits, DFAFCs have two major drawbacks that limit its lifetime and efficiency; the poor electrocatalytic activity (due to CO and Halides poisoning) and stability of the Pt-based electrodes. Herein, the electrocatalytic activity, stability and tolerance against poisoning species (CO and Halides) of Pt-based electrode (Pt/GC) towards formic acid (FA) oxidation; essential anodic reaction of DFAFCs, are shown to increase via interrupting the Pt surface with gold nanoparticles (AuNPs). Electrochemical measurements show that gold nanopartciles (AuNPs) modified Pt/GC (Au/Pt/GC) electrode supports a significant enhancement on the direct FA oxidation to CO_2 (the dehydrogenation pathway). On the other hand, the oxidative treatment of GC (GC_{ox}) in acidic medium results in 2 times increases on the catalytic activity of unmodified and AuNPs modified Pt electrodes towards direct FA oxidation to CO_2 compared to un-oxidized GC electrode. This significantly enhanced activity of AuNPs modified Pt/GC catalysts can be attributed to noncontiguous arrangement of Pt sites in the presence of the neighbored AuNPs, which promotes direct oxidation of FA to CO_2 and retards the adsorption of CO at Pt surface. Moreover, AuNPs modified Pt/GC catalyst has satisfactory stability and show high tolerance against halides poisoning.

G.A. El-Nagar (✉) · A.M. Mohammad · M.S. El-Deab · B.E. El-Anadouli (✉)
Chemistry Department, Faculty of Science, Cairo University, Cairo 12613, Egypt
e-mail: Gumaa@sci.cu.edu.eg

B.E. El-Anadouli
e-mail: bahgat30@yahoo.com

A.M. Mohammad
e-mail: ahmad.mohammad@bue.edu.eg

M.S. El-Deab
e-mail: msaada68@yahoo.com

A.Y. Oral et al. (eds.), *2nd International Congress on Energy Efficiency and Energy Related Materials (ENEFM2014)*, Springer Proceedings in Energy,
DOI 10.1007/978-3-319-16901-9_46

1 Introduction

Fuel cells (FCs) have received growing attention as they have been proved efficient, eco-friendly, reliable, quiet, long-lasted, easily installed and moved, economic and perfect for residential, and transportation uses and portable electronic applications. Of these, the DFAFCs are attractive candidate to replace methanol and hydrogen fuel cells as a promising candidate for portable and mobile applications, due to the unique advantages of FA as a fuel [1, 2]. Nevertheless, DFAFCs experience a severe problem where the catalytic activity of the Pt anodes, on which the FA electro-oxidation (FAO) proceeds, ceases with time, due to the accumulation of the poisoning CO intermediate resulting from the "*non-faradaic*" dissociation of FA (i.e., dehydration pathway) [3–5]. Therefore, the development of efficient and stable anodes overcoming the CO poisoning for FAO is a central issue. Another grave concern challenging the commercialization of FCs is the electrolyte's contamination with hydrocarbons (released from piping, blowers, pumps and heat exchangers) and species of a high adsorption tendency such as halides (where most of the high-surface area FCs catalysts are often synthesized from halide-containing educts) [6–9]. Herein, we report on the superior electrocatalytic activity, stability and the tolerance of a bimetallic modified GC electrode with gold nanoparticles (AuNPs) and platnium nanoparticles (PtNPs) toward the electrooxidation of FA.

2 Experimental

Glassy carbon (GC, d = 3.0 mm) electrode served as the working electrodes. An Ag/AgCl/KCl (sat) and a spiral Pt wire were used as reference and counter electrodes, respectively. PtNPs and AuNPs were electrodeposited on polished (assigned as GC) or electrochemically treated GC (assigned as GCox) surfaces as describe elsewhere [2–6]. The electrochemical treatment of polished GC electrode was performed by anodic polarization in 0.5 M H_2SO_4 at 2.25 V for various times [10]. The real surface area of platinum deposit (A_{Pt}) was estimated using the charge of Hydrogen adsorption/desorption in cyclic voltammograms (from −0.2 to 0.15 V) of Pt/GC and Pt/GC_{ox} electrodes, see Table 1 [2–6]. The electrocatalytic activities of the prepared electrodes

Table 1 Parameters of Pt/GC electrodes with different oxidation times prior to Pt deposition

Electrode, oxidation time (s)	Pt loading W_{Pt} (μg/cm^2)	Pt surface area A_{Pt} (cm^2)	Specific catalyst area S_{Pt} (m^2/g)	Q_{direct}/mC	$Q_{indirect}$/mC
Pt/GC, 0.0 s	65.50	0.633	13.8	0.4	2.3
Pt/GC_{ox}, 5.0 s	66.11	0.789	17.0	0.7	1.3
Pt/GC_{ox}, 10 s	65.92	0.982	21.3	1.0	1.0
Pt/GC_{ox}, 20 s	64.89	1.325	29.2	1.2	0.8
Pt/GC_{ox}, 30 s	67.12	1.553	33.1	1.5	0.5
Pt/GC_{ox}, 40 s	65.87	1.632	35.4	2.0	0.3

toward FAO are examined in an aqueous solution of 0.3 M FA. All measurements were performed using an EG&G potentiostat (model 273A) operated with Echem 270 software. A field emission scanning electron microscope, FE-SEM, (QUANTA FEG 250) coupled with an energy dispersive X-ray spectrometer (EDAX) unit was employed to evaluate the electrode's morphology and surface composition.

3 Results and Discussion

3.1 Material and Electrochemical Characterizations

Figure 1A, B depicts that oxidation of GC leads to a formation and growth of oxide layer, causing higher roughness and more defects on the surface as indicated from the EDAX analysis (see inset of each image). on the other hand, Figure 1C, D shows that PtNPs were electrodeposited at the GC (Fig. 1C) and GCox (Fig. 1D) surface in spherical crystallite aggregates with an average particle size of ca. 70 and 45 nm,respectively.

Furthermore, AuNPs have a flower-shaped geometry with an average particle size of ca. 100 nm for Au/GC electrode (Fig. 1E) and have a nano-wires like structures with average particle size 80 nm for Au/GCox electrode (Fig. 1F). Interestingly, the deposition of AuNPs on Pt/GC and Pt/GCox surfaces resulted in a decorated nanowire and a core-shell structures that homogeneously covered the entire surface of the GC electrode for Au/Pt/GC (Fig. 1G) and Au/Pt/GCox (Fig. 1H) electrodes, respectively. EDAX analysis showed the oxygen amount increased after the electrochemical treatment of the GC in acidic medium

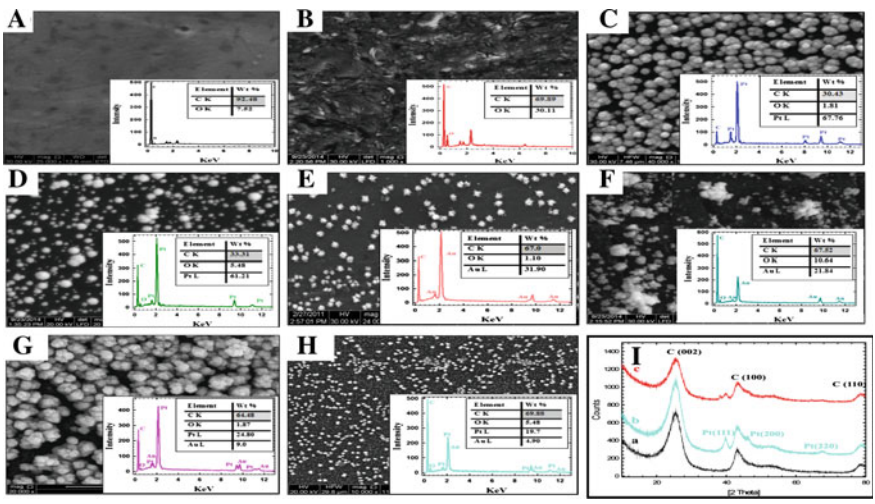

Fig. 1 FE-SEM images of **A** GC, **B** GC_{ox}, **C** Pt/GC, **D** Pt/GC_{ox}, **E** Au/GC, **F** Au/GC_{ox}, **G** Au/Pt/GC and **H** $Au/Pt/GC_{ox}$ (inset shows the EDAX analysis of each electrode). **I** XRD pattern of GC (*a*), Pt/GC (*b*) and Au/Pt/GC (*c*) electrodes

(insets of Fig. 1). Furthermore, the crystal structures of prepared GC, Pt/GC and Au/Pt/GC electrodes were studied using XRD as shown in Fig. 1I. All electrodes showed a broad peak at about $2\theta = 25°$ which is associated with carbon support (002). From the other hand, Pt/GC (curve b) and Au/Pt/GC (curve c) electrodes show the typical characteristic peaks for Pt (110), (200), (220), and (311), which demonstrates that the catalyst has a face-centered cubic (fcc) structure [2–6]. Bare Pt (Fig. 2A (curve a)) and Pt/GC (Fig. 2A (curve b)) electrodes show a typical CV of clean poly-crystalline Pt electrode [2–6]. Polished GC (Fig. 2A(g)) has no features under the experimental conditions, while oxidized GC (GC_{ox}) show redox peak at 0.4 V, related to the redox reaction quinon/hydroquinon in acidic solution (Fig. 2B (g')) [10]. Pt/GC_{ox} (Fig. 2B (curve b')) electrode reveal that characteristic peaks for Pt and oxidized GC are present at the same potentials as corresponding peaks at GCox and at Pt. Same behaviors obtained for Au/GC (Fig. 2A(c)) and Au/GCox (Fig. 2B(c')). Interestingly, upon electrodeposition of AuNPs on Pt/GC (assigned as Au/Pt/GC, Fig. 2A(e)) or Pt/GCox (assigned as Au/Pt/GCox, Fig. 2B (e')) electrodes, PtO reduction peak around ca. 0.48 V decrease but still can be

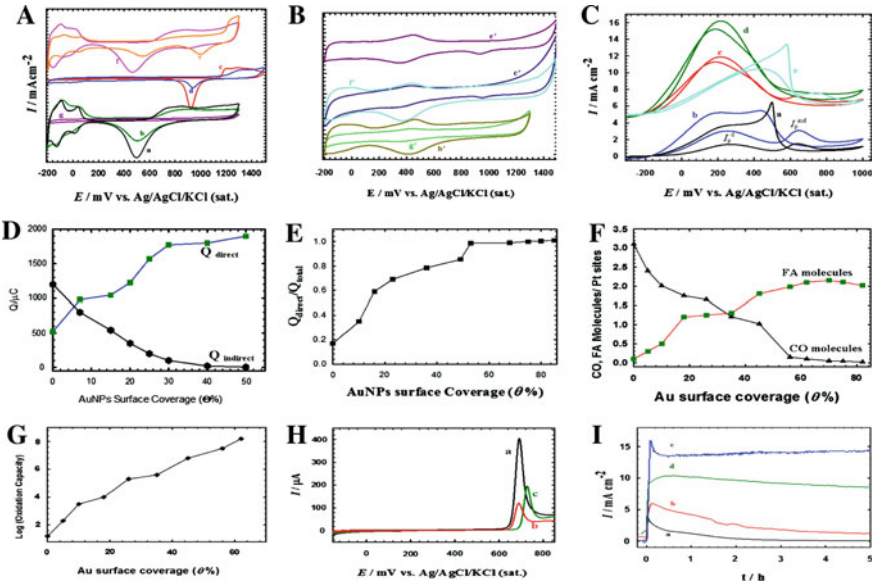

Fig. 2 **A** and **B** CVs in 0.5 M H_2SO_4 for (*a*) bare Pt, (*b*)Pt/GC ((*b'*) Pt/GC_{ox}), (*c*) bare Au, (*d*) Au/GC ((*d'*)Au/GC_{ox}), (*e*) Au/Pt/GC ((*e'*) Au/Pt/GC), (*f*) Pt/Au/GC ((*f'*) Pt/Au/GC_{ox}) and (*g*) GC bare ((*g'*) GCox) electrodes at 100 mVs^{-1}. **C** FAO at (*a*) Pt/GC, (*b*) Pt/GC_{ox}, (*c*) Au/Pt/GC, (*d*) Au/Pt/GC_{ox} and (*e*) Pt/Au/GC electrodes in 0.3 M FA in 0.5 M H_2SO_4. **D** Variation of Q_{direct} and $Q_{indirect}$, **E** Variation of Q_{direct}/Q_{total} with AuNPs surface coverage, **F** number of CO and FA molecules per active PtNPs sites and **G** Log oxidation capacity (*OC*) of direct FAO with AuNPs surface coverage. **H** CO stripping at (*a*) Pt/GC, (*b*) Au/Pt/GC and *c* Pt/Au/GC in 0.5 M H_2SO_4 at 50 mV s^{-1}. **I** *i-t* obtained during FAO at (*a*) Pt bare, (*b*) Pt/GC, (*c*) Au/Pt/GC and (*d*) Pt/Au/GC at +0.3 V

observed and the other oxide reduction peak appeared at ca. 0.9 V which corresponding to Au oxide reduction. A closer look at the evolution of the Au oxide reduction peak at ca. 0.9 V for Pt/Au/GC (Fig. 2A(f)) and Pt/Au/GCox (Fig. 2B(f')) electrodes reveals that the complete disappearance of the Au oxide reduction peak when PtNPs were electrodeposited on modified Au/GC or Au/GCox, while the PtO reduction peak still exist, when PtNPs were electrodeposited on modified Au/GC electrode suggests that the AuNPs are completely coated by the PtNPs and so a core-shell structure is formed but, on the other hand, the existing of the two peaks of Au and Pt oxide reduction peaks for Au/Pt/GC and Au/Pt/GCox means that the Au and Pt nanoparticles are exposed at the surface and so a decorated structure is obtained.

Electrocatalytic activity towards formic acid oxidation (FAO) A typical CV of FAO at was obtained at Pt/GC (curve a) and Pt/GC_{ox} (curve b) electrodes, where two oxidation peaks were observed in the forward direction, at ca. 0.23 (direct pathway I_p^d) and at 0.63 V (indirect or dehydration pathway, I_p^{ind}) [2–6, 11–13]. Figure 2C (curves a and b) reveals that Pt/GC_{ox} electrode has a higher electrocatalytic activity towards FAO than Pt/GC electrode with the same PtNPs loading, and the degree of enhancement increases with time of GC oxidation in acidic medium at 2.25 V (see Table 2.1). Thus, it is reasonable to assume that the main reason for enhanced activity of Pt/GC_{ox} regarding to Pt/GC is increased amount of reactive oxygen containing species (OH species) which leads to the lower coverage by CO_{ads} and permit the dehydrogenation path to increase in rate. Interestingly, upon electrodeposition of AuNPs on Pt/GC (Fig. 2C (curve c)) or Pt/GC_{ox} (Fig. 2C (curve d)) surfaces results in almost disappear of the I_p^{ind} (CO poising peak) with concurrent increases in the I_p^d (desirable peak) which means that FAO occurs exclusively via the dehydrogenation pathway instead of dehydration, and the Au/Pt/GC_{ox} has activity 2.0 times higher than that of Au/Pt/GC electrode with the same amount of AuNPs and PtNPs. Moreover, the degree of enhancement increase with AuNPs loading as indicated from the increase in direct FAO peak charge (Q_{direct}) and decrease charge of indirect FAO peak ($Q_{indirect}$) with AuNPs loading (see Fig. 2D). We believe that AuNPs interrupting the contiguity of Pt sites necessary for CO adsorption which leads to resist the formation of CO by which called ensemble effect [4, 5]. Moreover, the ratio between the direct FAO charge (Q_{direct}) and total FAO charge (direct and indirect); Q_{direct}/Q_{total}, increase with AuNPs surface coverage till $\theta \leq 57$ % and after that value this ratio remain constant at 1.0, which means that after that value FAO exclusively via dehydrogenation pathway (Fig. 2E). One fundamental issue, in the preparation of an efficient catalyst towards a target reaction, is the proper design of the catalyst with efficient use of its constituents specially the precious metal. In this context, it is essential to investigate the influence of the deposition sequence of PtNPs and AuNPs on the electrocatalytic performance toward FAO. Figure 2D(c&e) compares the CVs for FAO obtained at Au/Pt/GC (curve c) and Pt/Au/GC (curve e) electrodes. Obviously and as evident from these two curves, the deposition sequence of the two species influences the electrocatalytic activity towards FAO. That is, the activity obtained at Au/Pt/GC electrode was better than that obtained at its "*mirror image*" Pt/Au/GC electrode.

This can be explained in view of the necessity of a certain adsorption sites for FA and CO on Pt surface. The deposition of AuNPs as a topmost surface layer could interrupt this contiguity and eventually inspire a better electrocatalytic activity. In order to reveal the adsorption mode of FA onto the Pt surface at different θ, the number of adsorbed FA and CO molecules was estimated from the amount of charge consumed in the direct and in direct peaks, respectively, of FAO assuming 2-electron transfer processes (data are plotted in Fig. 2F) [6, 7]. Interestingly, Fig. 2F reveals the existence of two adsorption modes for FA onto the Pt surface. At low θ (≤ 40 %), every molecule of FA is bound to a single Pt site (the FA/Pt ratio is ~ 1) because of the availability of plenty active Pt sites for FAO. On the other hand, at high θ (≥ 40 %), the shortage in the available free Pt sites may stimulate another adsorption mode, in which two molecules of FA are likely adsorbed onto a single Pt site. A similar phenomenon has recently been observed for the adsorption of acrylonitrile onto nano-Pt/GC surfaces [6]. Note also the continuous reduction of the CO/Pt ratio (from 3 down to less than 0.5) with θ, which highlights the remarkable improvement in the catalytic tolerance of the Pt/GC electrode against the CO poisoning. We have recently developed another important index, "oxidation capacity (*OC*)", to probe the catalytic activity, which normalizes the charge consumed in the direct oxidation peak (Q_{direct}) to the number of available Pt active sites, as this ratio increase means that the electrode has more CO tolerance [6, 7]. Figure 2G shows that the oxidation capacity of the Au/Pt/GC electrode increases with surface coverage reach to about *8 order* of magnitude, however the deposition of AuNPs decrease the area of the Pt/GC electrode. The presence of AuNPs on the surface of PtNPs increase the number of active Pt sites available for direct FAO and decrease the number of active Pt sites for CO adsorption via third-body effect which leads to increase in oxidation capacity towards formic acid oxidation.

To test this, CO was adsorbed on bare Pt/GC, Pt/Au/GC and Au/Pt/GC electrodes and then oxidized in the CO-free electrolyte 0.5 M H_2SO_4 data are presented in Fig. 2H. As clearly seen in this figure, the Au/Pt/GC (curve b) and Pt/Au/GC (curve c) electrodes have less amount of CO than Pt/GC (curve a) as calculated from the charge used for CO stripping peaks at the three electrodes. The oxidation of CO_{ads} on Pt/Au/GC (curve c) is delayed for ~ 0.15 V with respect to Pt/GC (curve a) with less amount of CO formed which give an evident for presence of electronic interaction between AuNPs and PtNPs. This figure clearly shown that, the presence of Au does not facilitate CO oxidation at low potential, but due to resist the CO formation via interrupt the PtNPs contiguity surface (third-body effect). Figure 2I depict that Au/Pt/GC and Pt/Au/GC electrodes supports higher oxidation about 9.0 and 15 times current than that obtained at Pt/GC, respectively. This level of enhancement could still be observed after 5 h of continuous measurement. This again demonstrates the preference of the direct oxidation path of FA at the AuNPs modified Pt/GC electrodes and its high CO tolerance.

3.2 Temperature Effect and Halides Tolerance

Effort was further dedicated to evaluate the influence of halides ions (e.g., Cl^-, Br^- and I^-) prescence in the electrolyte of the anodic compartment of DFAFCs, which may act similarly as the poisonous CO, and the degree of tolerance of each electrode against it. Figure 3 shows the effect of existence halides ions on the effective surface area of Pt (ECSA) for the Pt/GC (Fig. 3a) and Au/Pt/GC (Fig. 3b) electrodes. These two figures depict that, (i) the presence of halides ions on the electrolyte of anodic compartment of DFAFCs resulted in a significant decrease on the ECSA of PtNPs, (ii) ECSA of PtNPs decrease with lower rate for Au/Pt/GC compared to Pt/GC electrode, for instance presence of 60 ppm of Cl, Br or I ions resulted in a completely poisoning the PtNPs surface (Fig. 3a), while same concentrations lead to only 38, 42 and 80 % decrease on the ECSA of PtNPs of Au/Pt/GC electrodes (Fig. 3b). We believe the different adsorption tendency of halide ions on Au and Pt is a key to understand this behavior, and soon we will continue the investigation to evaluate the essence of this issue, and (iii) the effect of halides on ECSA has the following order $Cl^- < Br^- < I^-$ and this expected behavior as the

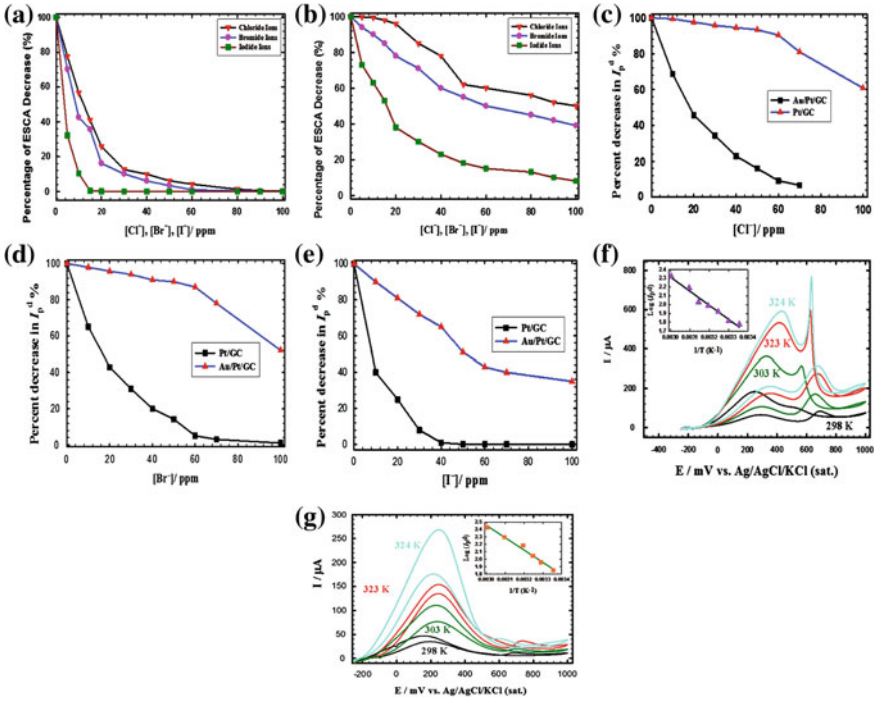

Fig. 3 Variation of ECSA of Pt in Pt/GC (**a**) and Au/Pt/GC (**b**) with halides concentrations. Percent decrease in the direct FAO peak (I_p^d %) with **c** chloride, **d** Bromide and **e** Iodide ions concentrations. Effect of temperature on FAO at **f** Pt/GC and **g** Au/Pt/GC electrodes (*inset* shows the Arrhenius plot)

difference in electronegativity, ionic radii and solvation ability between chloride and bromide ion. Figure 3 (C-E) compares the percent decrease in I_p^d as a function of the (C) Cl^-, (D) Br^- and (E) I^- ions concentration at both of the Pt/GC (black-squared lines) and Au/Pt/GC (red-triangle lines) electrodes. As obviously seen, the degrees of tolerance of the Au/Pt/GC electrodes against poisoning with halides (Cl^-, Br^-, I^-) are much better than that at the Pt/GC electrode at all concentrations of halides (Cl^-, Br^-, I^-) ions in the range investigated. For instance, the catalytic activity of the Au/Pt/GC electrode was reduced only to ca. 97, 95 and 50 % in 60 pm Cl^-, Br^- and I^- ions, respectively. While the same concentrations decreased the catalytic activity of Pt/GC electrode to about 2 % (see Fig. 3c–e). The solution temperature is another vital parameter in determining the catalytic performance of the proposed AuNPs modified Pt electrode. Figure 3g, f shows an increase of forward and backward current of FAO at Pt/GC (Fig. 3g) and Au/Pt/GC (Fig. 3g) electrodes with temperature up to 60 °C. An increase forward and backward current of FAO with temperature reflects a more favorable kinetics of the FAO at both potential scan directions. The value of an apparent activation energy (*Ea*) is calculated by plotting the current (*I*) at a specific potential as a function of temperature (*T* in *K*) according to Arrhenius equation (insets of Fig. 3 f, g). insets of Fig. 3f, g shows a representative Arrhenius plot for the oxidation of FA in which log *I* is plotted against T^{-1} at a potential of 0.2 V and the linear plot gives 20 and 16.2 kJ mol^{-1} as *Ea* for Pt/GC and Au/Pt/GC, respectively, and that result can be explained why Au/Pt/GC electrode has a higher electrocatalytic activity towards FAO compared to Pt/GC electrodes.

4 Conclusion

The current investigation addresses the development of a binary PtNPs and AuNPs catalyst for the efficient FAO. A mechanistic interpretation for the catalytic activity assumed the necessity of Pt surface sites for the adsorption of FA. The deposition of AuNPs on the Pt/GC electrode interrupted the contiguity of the Pt sites, which is necessary for the CO adsorption. The Au/Pt/GC electrode showed an excellent stability and tolerance against the poisoning effect of halides ions than Pt/GC electrode. The electrochemical treatment of GC before PtNPs deposition resulted in 2 times higher on the catalytic activity of Pt/GC electrode towards FAO.

References

1. X. Yu, P.G. Pickup, Recent advances in direct formic acid fuel cells (DFAFC). J. Power Sources **182**(1), 124–132 (2008)
2. G.A. El-Nagar, A.M. Mohammad, M.S. El-Deab, B.E. El-Anadouli, Facilitated electrooxidation of formic acid at nickel oxide nanoparticles modified electrodes. J. Electrochem. Soc. **159**(7), F249–F254 (2012)

3. G.A. El-Nagar, A.M. Mohammad, M.S. El-Deab, B.E. El-Anadouli, Electrocatalysis by design: Enhanced electrooxidation of formic acid at platinum nanoparticles–nickel oxide nanoparticles binary catalysts. Electrochim. Acta **94**(1), 62–71 (2013)
4. G.A. El-Nagar, A.M. Mohammad, Enhanced electrocatalytic activity and stability of platinum, gold, and nickel oxide nanoparticles-based ternary catalyst for formic acid electro-oxidation. Int. J. Hydrogen Energy **39**(23), 11955–11962 (2014)
5. G.A. El-Nagar, A.M. Mohammad, M.S. Mohamed, B.E. El-Anadouli, Electro-oxidation of formic acid at binary platinum and gold nanoparticle-modified electrodes: effect of chloride ions. Int. J. Electrochem. Sci. **9**, 4523–4534 (2014)
6. G.A. El-Nagar, A.M. Mohammad, M.S. El-Deab, T. Ohsaka, B.E. El-Anadouli, Acrylonitrile-contamination induced enhancement of formic acid electro-oxidation at platinum nanoparticles modified glassy carbon electrodes. J. Power Sources **265**(1), 57–61 (2014)
7. M.S. El-Deab, A.M. Mohammad, G.A. El-Nagar, B.E. El-Anadouli, Impurities contributing to catalysis: enhanced electro-oxidation of formic acid at Pt/GC electrodes in the presence of vinyl acetate. J. Phys. Chem. C **118**(39), 22457–22464 (2014)
8. M.S. El-Deab, F. Kitamura, T. Ohsaka, Impact of acrylonitrile poisoning on oxygen reduction reaction at Pt/C catalysts. J. Power Sources **229**(1), 65–71 (2013)
9. M.S. El-Deab, F. Kitamura, T. Ohsaka, Poisoning effect of selected hydrocarbon impurities on the catalytic performance of Pt/C catalysts towards the oxygen reduction reaction. J. Electrochem. Soc. **160**(6), F651–F658 (2013)
10. V.M. Jovanović, D. Tripković, A. Tripković, A. Kowal, J. Stoch, Oxidation of formic acid on platinum electrodeposited on polished and oxidized glassy carbon. Electrochem. Commun. **7** (10), 1039–1044 (2005)
11. J. Joo, T. Uchida, A. Cuesta, M.T.M. Koper, M. Osawa, Importance of acid-base equilibrium in electrocatalytic oxidation of formic acid on platinum. J. Am. Chem. Soceity **135**(1), 9991–9994 (2013)
12. J. Joo, T. Uchida, A. Cuesta, M.T.M. Koper, M. Osawa, The effect of pH on the electrocatalytic oxidation of formic acid/formate on platinum: a mechanistic study by surface-enhanced infrared spectroscopy coupled with cyclic voltammetry. Electrochim. Acta **129**, 127–136 (2014)
13. G. Samjeské, A. Miki, S. Ye, M. Osawa, Mechanistic study of electrocatalytic oxidation of formic acid at platinum in acidic solution by time-resolved surface-enhanced infrared absorption spectroscopy. J. Phys. Chem. B **110**, 16559–16566 (2006)